Direct photon measurements with the ATLAS and CMS detectors

Marcos Jimenez Belenguer (on behalf of ATLAS and CMS)

Outline

- ❑ Introduction and motivation
- ❑ Photon reconstruction and identification performance
- ❑ Background suppression (shower shapes and isolation)
- ❑ Background decomposition (templates and sidebands)
- ❑ Physics measurements
  - → Inclusive photon differential cross section
    - PDF constraints
  - → Dynamics of photon-jet events and photon-jet differential cross section
    - PDF constraints
  - → Di-photon differential cross sections
- ❑ Conclusions

Photons at LHC – introduction and motivation

- LO direct photon production at the LHC

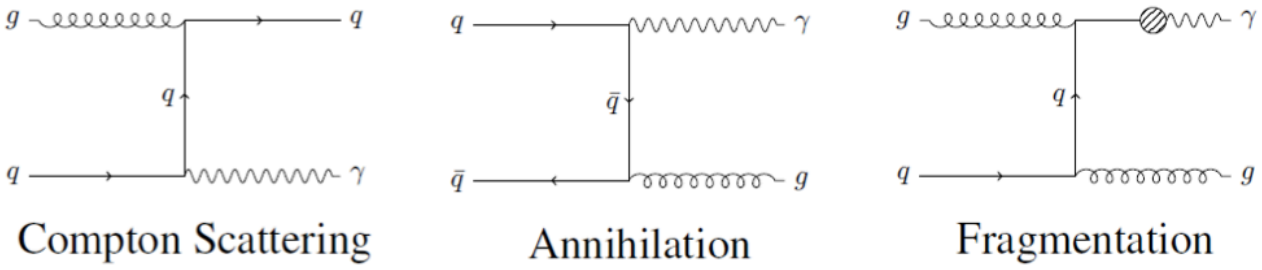

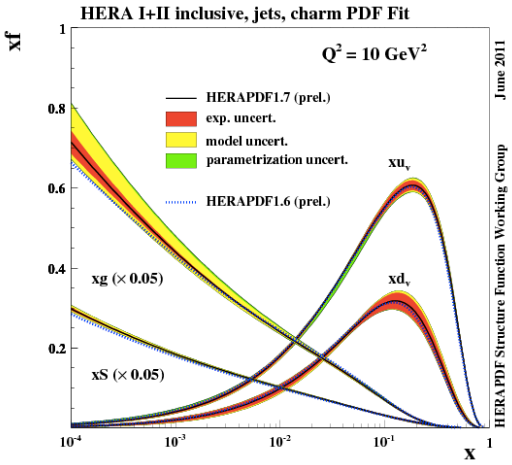

→ *Compton scattering dominant at LO due to prevalence of gluon PDF at low x for LHC √s*

- **Measurements of isolated photon production provide a powerful testing ground for pQCD**
  - → **Test of QCD predictions with colorless (clean) final state**
  - → **Large Compton Scattering contribution probes gluon PDF and can help reduce its uncertainty when included in global QCD fits *(i.e. reduce one of main sources of theoretical uncertainty in many LHC analyses)***
  - → **photon-jet measurements are useful for performance studies (i.e. jet-energy calibration)**
  - → **photon-jet and photon-photon processes are the dominant backgrounds in new physics searches (i.e. H→2photons, gravitons, exited fermions, SUSY, etc…)**

Photon reconstruction

- **Photons initiate em shower in ECAL**

→ *reco algorithms search for ECAL cell clusters with significant energy*

- **Photons may convert in inner detector (proportional to amount of material)**

→ *not matched to tracks (unconverted)*

→ *2 & 1 track matching for converted γ*

- **Some inherent ambiguity left between electrons and photons**

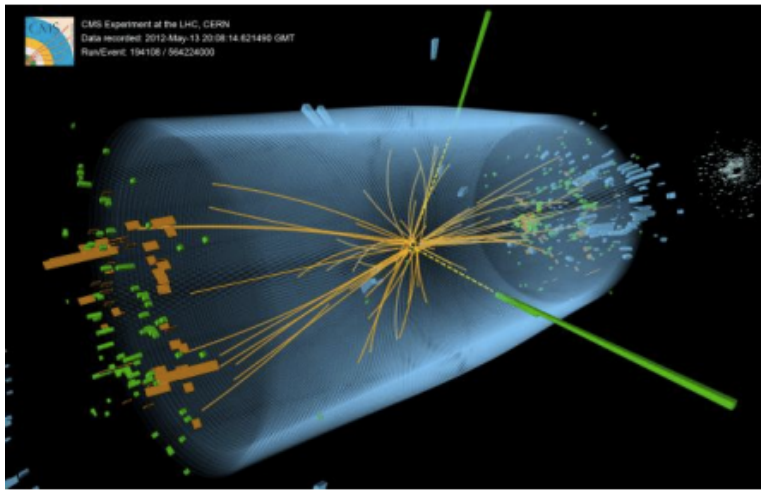

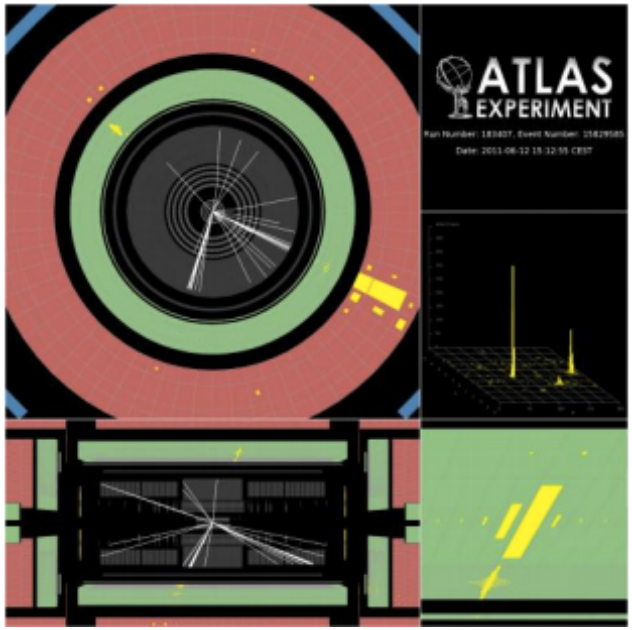

Background suppression - isolation

- QCD jet production is orders of magnitudes above the signal

→ *Jets dominated by light neutral meson that decays to collimated photons constitute dominant photon background - **Large background rejection needed !***

- **Isolation is applied at tracking, ECAL and HCAL level**

→ **For ECAL isolation ($\Delta R<0.4$) criteria (also used at generator level for comparisons to theory prediction)**

- **ISO = iso_{track} + iso_{EMC} + iso_{HCAL}**
  - **Signal and background shapes are very different**
  - **EMAC Isolation is a good discriminant variable**

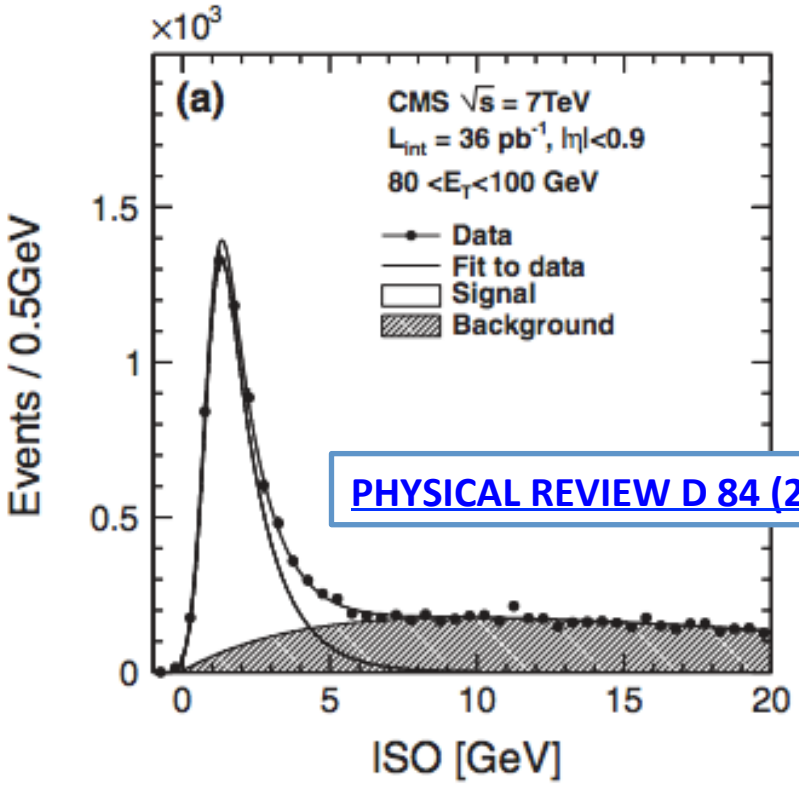

PHYSICAL REVIEW D 84 (2011) 052011

Background suppression - isolation

→ Isolation largely suppresses the fragmentation contribution (although still significant at low pT)

→ ***This makes theoretical predictions more reliable***

Before isolation

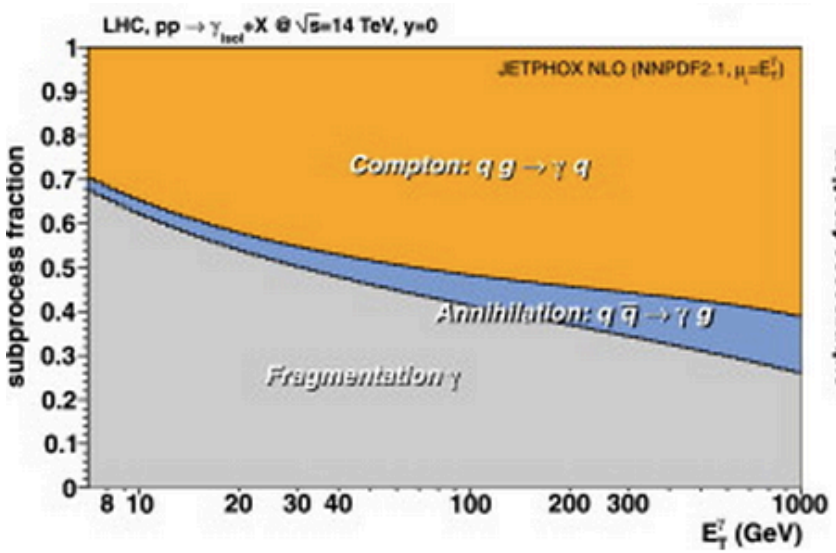

After isolation

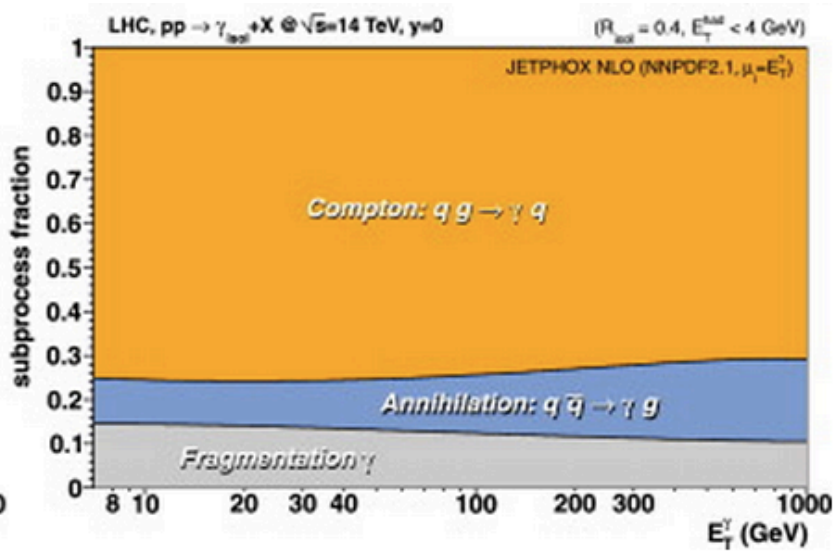

Nucl.Phys. B860 (2012) 311-338

Background suppression – shower shapes

- QCD jet production is orders of magnitudes above the signal

→ *Jets dominated by light neutral meson that decays to collimated photons constitute dominant photon background - **Large background rejection needed !***

- Both ATLAS and CMS exploit the granularity of the detector to reject background based on the shapes of the electromagnetic shower

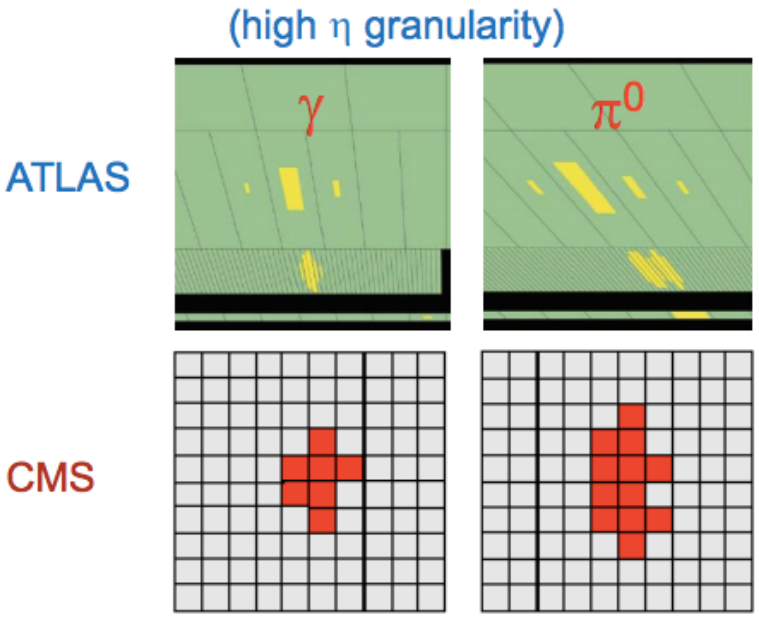

ATL-COM-PHYS-2013-244

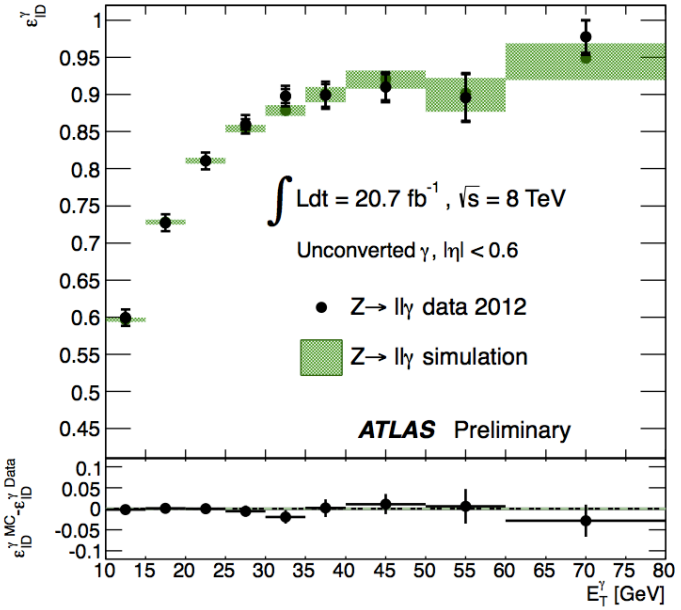

Background decomposition (data-driven)

- ***Both CMS and ATLAS exploit isolation as a discriminant variable to perform background decomposition in inclusive photon, photon-jet and photon-photon analyses***
- **Methods used include : 1-D Sideband, template fits, 2-D sidebands, event weights**
  → ***cross-check using E_T/p_T for converted photons (CMS)***

- ATLAS higher purity at low pT (at the expense of lower effiency- previous slide)

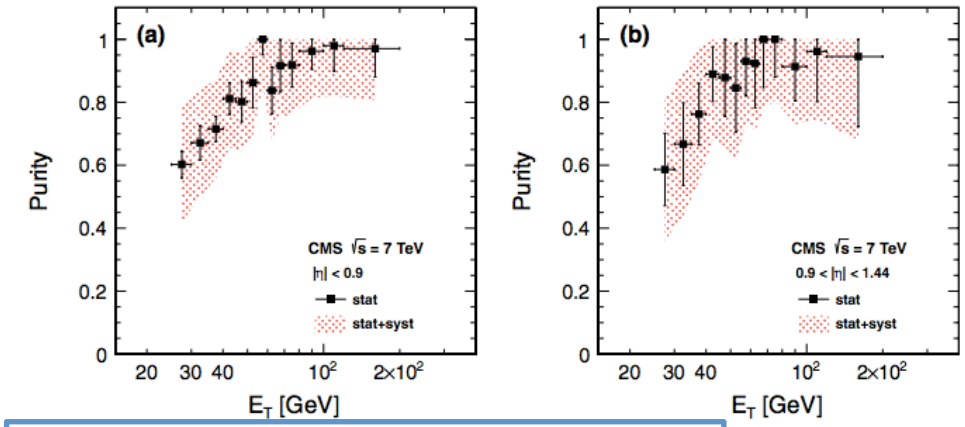

PHYSICAL REVIEW D 84 (2011) 052011

PHYSICAL REVIEW D 83, 052005 (2011)

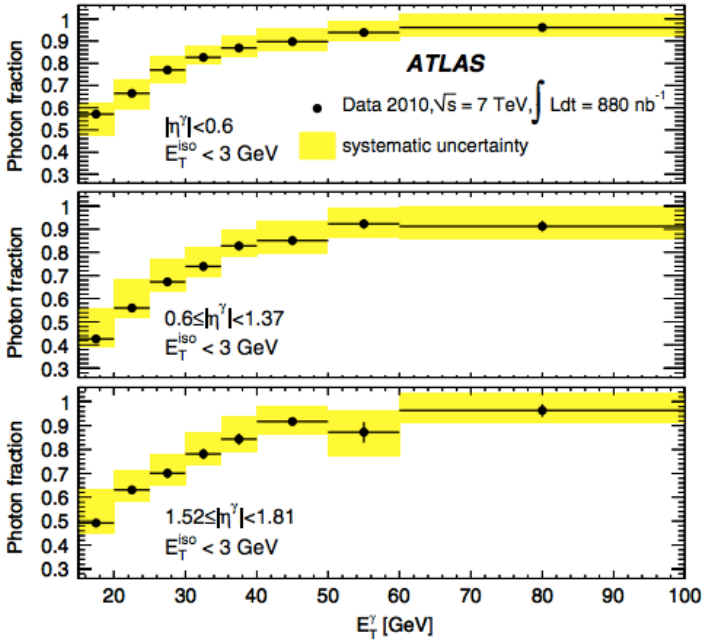

Results - Inclusive photon cross-sections vs E_T

- ❑ PID efficiency and background estimate are dominant experimental uncertainties
- ❑ Data compared to JETPHOX NLO pQCD
- ➢ Highest disagreement at low ET
- ➢ Large PDF (gluon) uncertainties at ET>700 GeV PYTHIA in good agreement with data
- ➢ HERWIG systematically lower but within errors

ATL-PHYS-PUB-2011-013 ~35 pb^{-1}

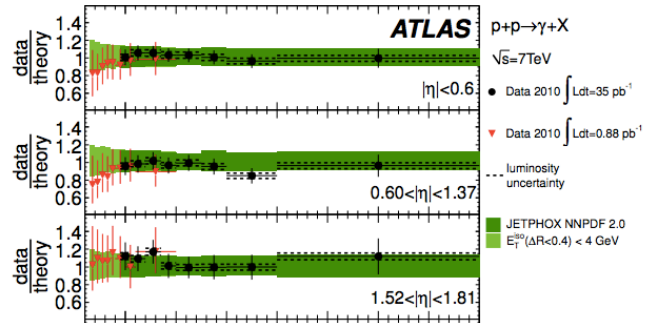

PHYSICAL REVIEW D 84 (2011) 052011 ~36 pb^{-1}

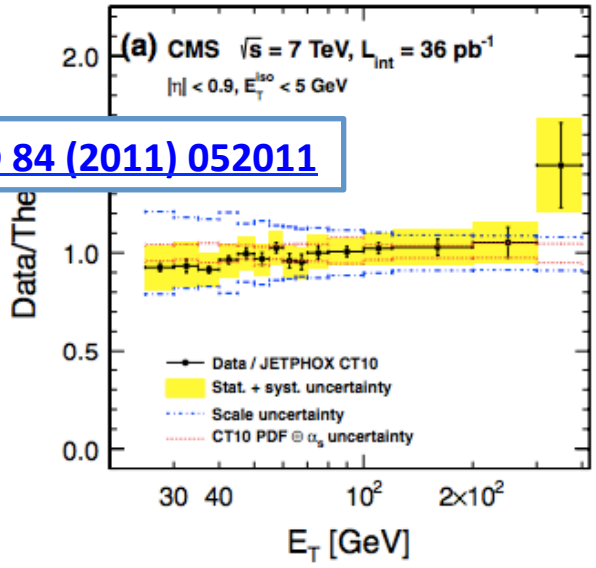

ATLAS-CONF-2013-022

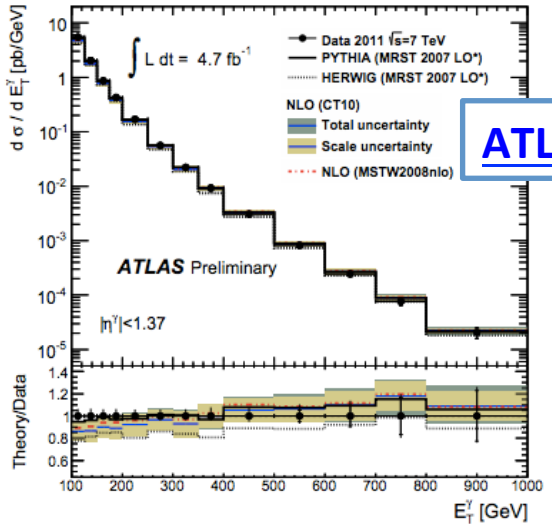

- ❑ Adding LHC 2010 measurements together with RHIC, SppS, Tevatron

→ **up to 20% gluon PDF uncertainty reduction!** *Nucl.Phys. B860 (2012) 311-338*

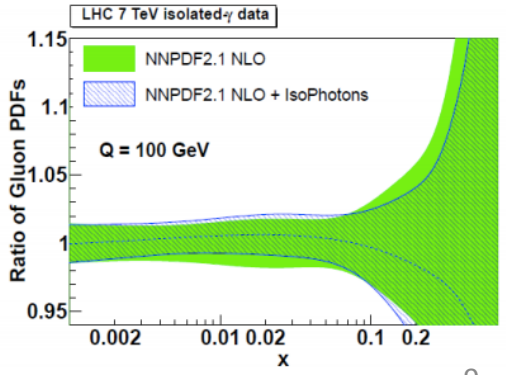

Photon-jet measurements

CMS PAS QCD-11-005

- **Angular distributions probe:**
  - → **different x regions (help constraint q/g PDFs) →**
  - → **direct-to-fragmentation composition**

- ATLAS and CMS comparison of data to JETPHOX
- → Same feature at low E_T as for inclusive photon analysis – otherwise fair agreement
- → Sherpa (higher order ME + PS) also compared in CMS case – tends to undershoot LHC data (while in agreement with Tevatron data)

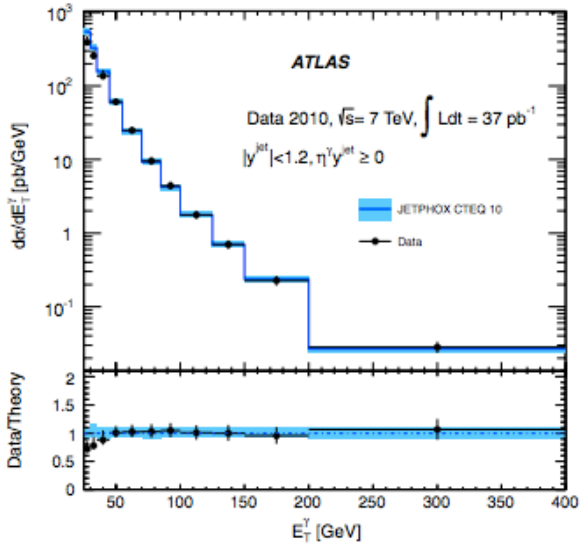

L=37 pb^{-1}
Jet P_T > ~20 GeV

CERN-PH-TH/2013-006

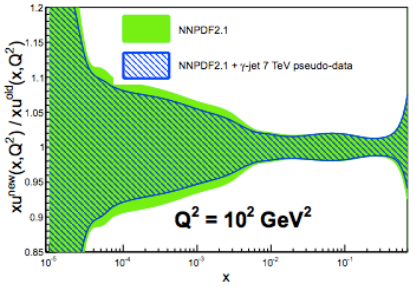

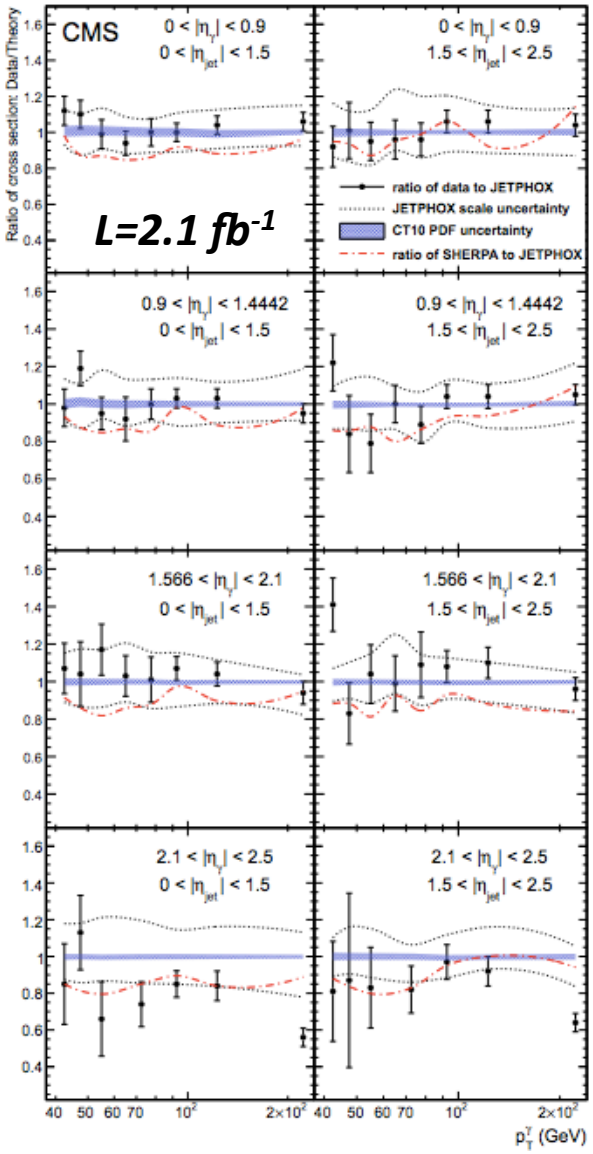

PHYSICAL REVIEW D 85, 092014 (2012)

Photon-jet dynamics

- **Measurements of differential cross sections for photon-jet (photon E_T > 45 GeV) are measured and regions of particular sensitivity to DP/frag component are identified (35 pb^{-1} of √7 TeV data)**
- **$m_{jet\text{-}gamma}$ and cos θ* distributions are studied**

$$\cos\theta^* = 2\, p_{T\gamma 1}\, p_{T\gamma 2} \sinh(\eta_{\gamma 1}-\eta_{\gamma 2})/(m_{\gamma\gamma}\, m_{T\gamma\gamma})$$
[Collins-Soper]

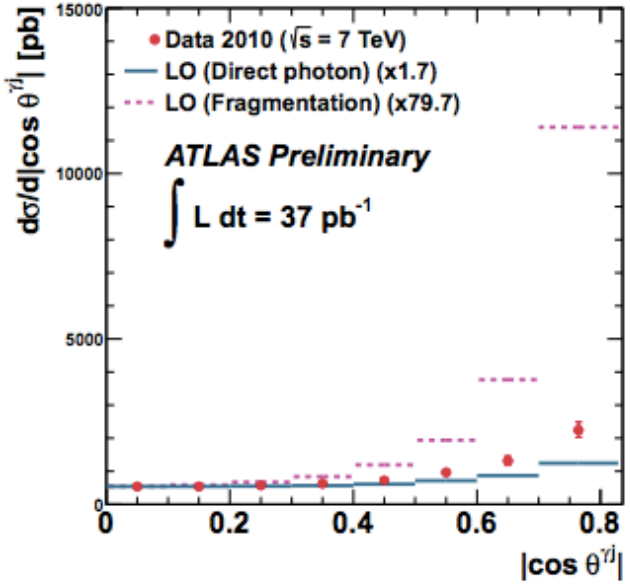

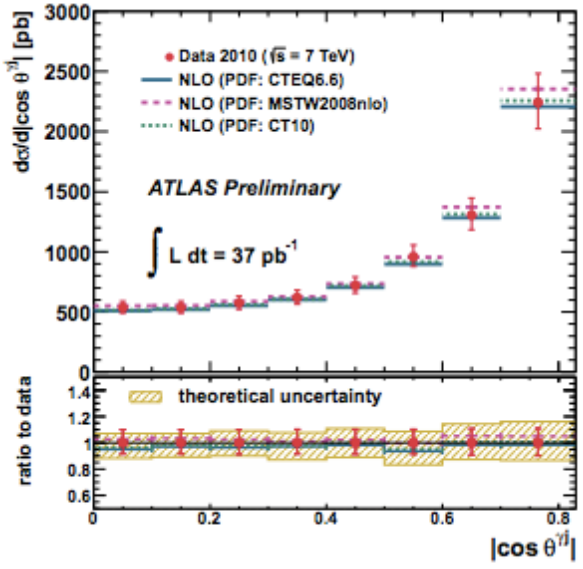

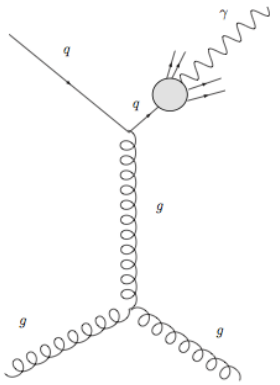

Fragmentation dominated by spin 1, whereas DP is dominated by spin ½ interchange

- Different shapes of DP and frag events for **cos θ* are due to spin structure of exchanged particle** → **data show dominance of QCD Compton Scattering**

Photon-photon differential cross sections

- Both ATLAS and CMS have measured the di-photon differential cross section as a function of $\Delta\Phi_{\gamma\gamma}$ $m_{\gamma\gamma}$ $p_{T\gamma\gamma}$ and $|\cos\theta^*|$ using 4.9 fb^{-1} (~36pb^{-1}) of 7 TeV data, respectively
- **SM di-photons constitutes the main background in SM H→ di-photon searches**

JHEP01(2012)133

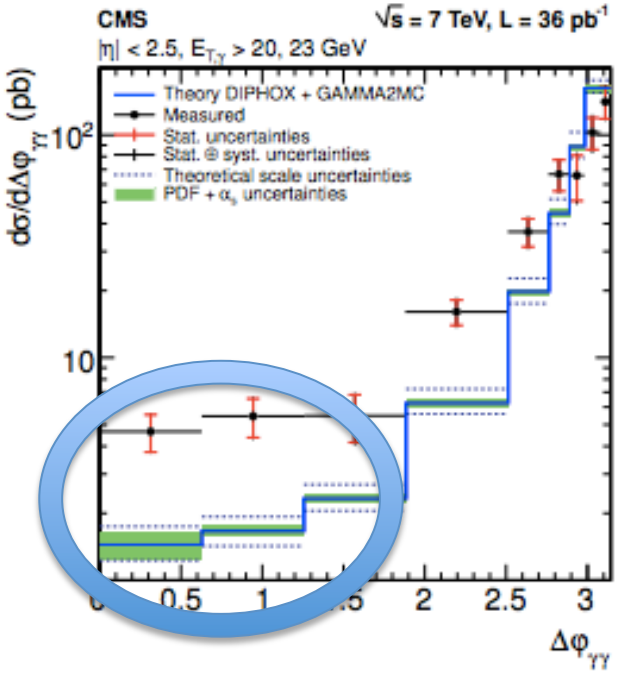

- **At LO the photons are back-to-back so higher order contributions at low $\Delta\Phi_{\gamma\gamma}$**

JHEP01(2013)086

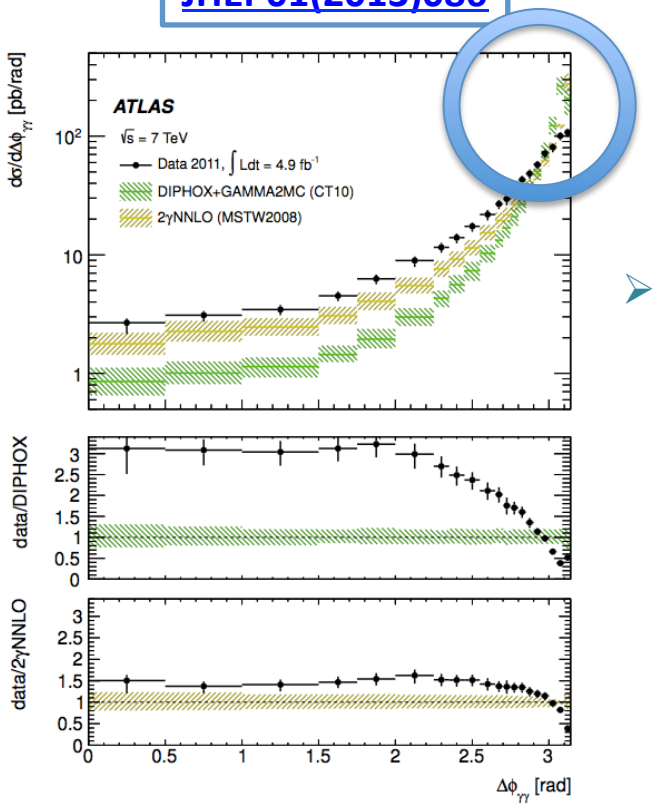

- **At high $\Delta\Phi_{\gamma\gamma}$ infrared divergences at fixed order** give higher DIPHOX predictions (PYTHIA and SHERPA do better there thanks to resummation at all orders of leading logs in the Parton Shower)

Photon-photon differential cross sections

- SM di-photons constitutes the main background in SM H→ di-photon searches

[JHEP01(2013)086]

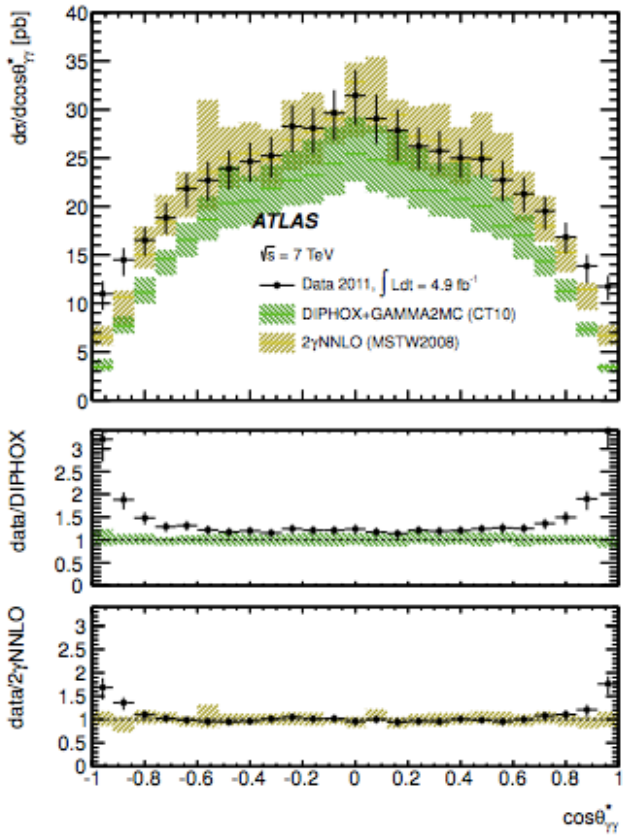

Slightly different variants of cos θ* but similar results

ATLAS $\cos\theta^* = 2\, p_{T\gamma 1}\, p_{T\gamma 2} \sinh(\eta_{\gamma 1}-\eta_{\gamma 2})/(m_{\gamma\gamma}\, m_{T\gamma\gamma})$ [Collins-Soper]

CMS $|\cos\theta^*| = |\tanh\frac{\Delta y_{\gamma\gamma}}{2}|$

- Generators tend to under-estimate the data at high cos θ*
  → **Fragmentation enhanced region**

Photon-photon differential cross sections

- SM di-photons constitutes the main background in SM H→ di-photon searches

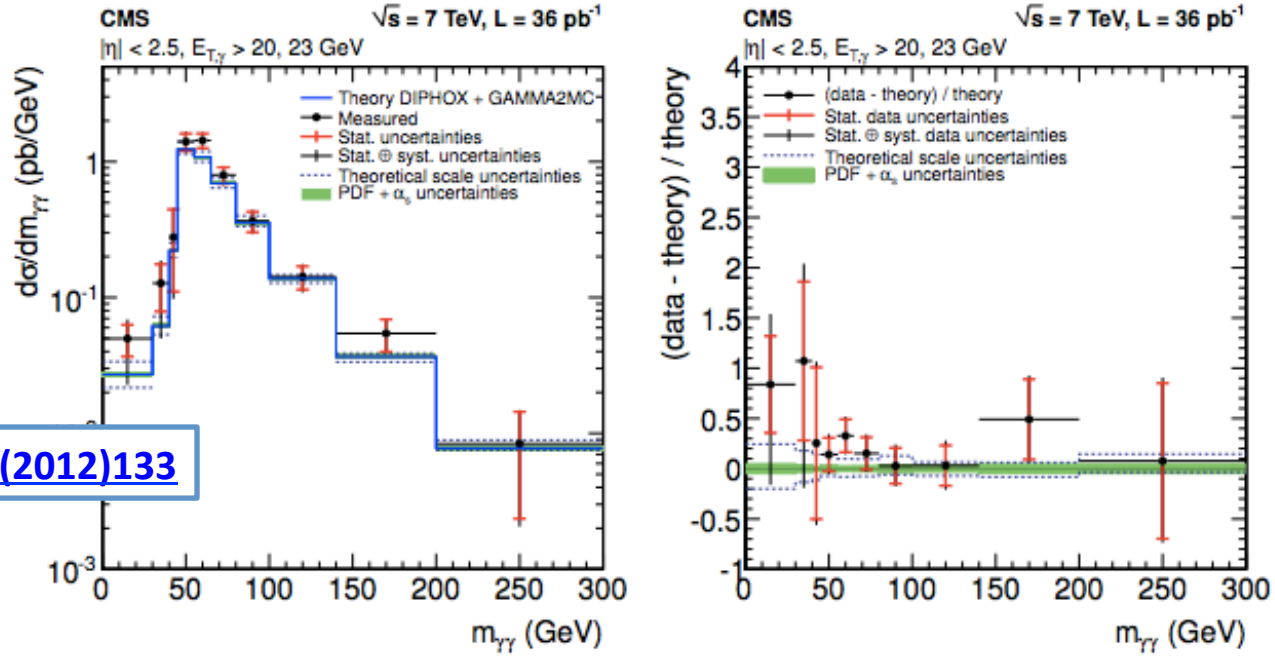

JHEP01(2012)133

- Deficit at low $m_{\gamma\gamma}$ is consistent with $\Delta\Phi_{\gamma\gamma}$ tail deficit
- **Otherwise very fair agreement (similar for ATLAS)**

Conclusions

- Measured photon differential cross sections are in good agreement with Monte-Carlo generators and fixed order calculations.
  → Highest disagreement found at low pT (< 40 GeV)

- Constraints on gluon PDF from LHC photon data are promising (up to 20% uncertainty reduction on gluon PDF from prompt photons)

- Potential for gluon and light quark PDF reduced uncertainties using latest photon-jet measurements

- **New results in 2013:**

  - Measurement of the di-photon cross-section with ATLAS 4.9 fb-1 @ 7 TeV, 2011 dataset, published January 2013, JHEP01(2013) 086

  - Measurement of the triple differential photon-jet cross-section with CMS 2.14 fb-1 @ 7 TeV 2011 dataset, CMS-PAS-QCD-11-005

  - Measurement of photon-jet dynamics (37 pb-1) with ATLAS, ATLAS-CONF-2013-023

  - Prompt photon cross section (4.7 fb-1) with ATLAS, ATLAS-CONF-2013-022

BACKUP - Dominant systematic uncertainties – CMS – inclusive photons (similar for ATLAS for isolation method (lower bkg uncertainties))

TABLE V. Systematic uncertainties expressed in percent for each source in the four η regions. The ranges, when quoted, indicate the variation over photon E_T. The unfolding correction is discussed in Sec. IX.

Source	$\|\eta\| < 0.9$	$0.9 < \|\eta\| < 1.44$	$1.57 < \|\eta\| < 2.1$	$2.1 < \|\eta\| < 2.5$
		Common		
Luminosity	4.0		4.0	
Energy scale	4.0		4.0	
Trigger efficiency	0.1		0.7	
		Photon conversion method		
Isolation efficiency	5.2	5.2	5.4	5.4
Conversion efficiency	11	11	8.9	8.9
Fit bias	0–4.1	0–6.1	0.1–4.2	0–5.3
Signal shape	1	2.3	3	3.1
Background shape	0.1–4.8	4.1–5.9	0.3–14	6.2–15
Electron background	0.01–0.1	0.02–0.2	0.05–1.1	0.03–0.8
Unfolding correction	4.0	4.0	4.0	4.0
Total	14–18	14–20	12–21	13–23
		Isolation method		
Efficiency	3.6–7.6	3.6–7.6	8.6	8.6
Fit bias	0.1–2.9	0.1–2.8	0.1–4.0	1.1–4.7
Signal/background shape	1.8–13	1.6–32	4.9–16	7.0–21
N^γ for E_T = 300–400 GeV	4.5	8.3	10	20
Electron background	<0.1	<0.1	<0.1	<0.1
Unfolding correction	2.0	2.0	2.0	2.0
Total	3.8–18	3.9–35	8.7–18	10–23

BACKUP - Dominant systematic uncertainties – gamma-jet

Table 1: Contributions to the relative systematic uncertainty (in percent) of the cross section from efficiency, unfolding, and purity calculations. The total systematic uncertainty is obtained by adding all contributions in quadrature. The numbers in the table represent the ranges of uncertainties obtained in different η^{γ} and η^{jet} bins. An additional 2.2% luminosity uncertainty is not included.

$\lvert\eta^{\gamma}\rvert < 1.4442$				
P_T^{γ} GeV	efficiency (%)	unfolding (%)	purity (%)	total (%)
40-45	2.5	2.1	4.9 - 9.3	5.9 - 9.9
45-50	1.2	2.5	4.9 - 17.0	5.5 - 17.2
50-60	4.5	2.6	4.2 - 13.4	6.7 - 14.4
60-70	4.5	2.4	3.7 - 11.4	6.3 - 12.5
70-85	4.5	1.2	4.6 - 5.7	6.6 - 7.4
85-100	4.5	1.4	2.2 - 3.1	5.2 - 5.6
100-145	4.5	1.4	1.8 - 2.5	5.0 - 5.4
145-300	4.5	1.2	1.4 - 2.6	4.9 - 5.3
$1.556 < \lvert\eta^{\gamma}\rvert < 2.5$				
P_T^{γ} GeV	efficiency (%)	unfolding (%)	purity (%)	total (%)
40-45	3.0	2.1	6.9 - 9.9	7.8 - 10.5
45-50	3.5	2.5	8.6 - 37.5	9.6 - 37.7
50-60	5.0	2.6	7.2 - 24.5	9.1 - 25.1
60-70	5.0	2.4	7.0 - 12.4	9.0 - 13.5
70-85	5.0	1.2 - 5.0	10.0 - 13.3	11.3 - 15.1
85-100	5.0	1.4 - 5.0	2.8 - 4.6	5.9 - 8.0
100-145	5.0	1.4 - 4.0	2.8 - 6.3	5.9 - 8.2
145-300	5.0	1.2 - 2.1	2.9 - 5.1	6.1 - 7.3

BACKUP - Dominant systematic uncertainties – di-photons

$p_{T,\gamma\gamma}$	$d\sigma/dp_{T,\gamma\gamma}$	Statistical error		Systematic errors		Total error	
[GeV]	[pb/GeV]	high	low	high	low	high	low
[0, 2)	0.727	+0.022	−0.022	+0.057	−0.092	+0.061	−0.094
[2, 4)	1.75	+0.04	−0.04	+0.13	−0.23	+0.13	−0.23
[4, 6)	2.03	+0.04	−0.04	+0.15	−0.23	+0.15	−0.23
[6, 8)	1.88	+0.04	−0.04	+0.15	−0.21	+0.16	−0.21
[8, 10)	1.72	+0.03	−0.03	+0.13	−0.19	+0.14	−0.19
[10, 12)	1.40	+0.03	−0.03	+0.12	−0.16	+0.12	−0.16
[12, 14)	1.28	+0.03	−0.03	+0.10	−0.13	+0.11	−0.13
[14, 16)	1.122	+0.026	−0.026	+0.093	−0.114	+0.097	−0.117
[16, 18)	0.999	+0.024	−0.024	+0.086	−0.090	+0.090	−0.093
[18, 20)	0.810	+0.021	−0.021	+0.072	−0.076	+0.075	−0.079
[20, 25)	0.674	+0.012	−0.012	+0.056	−0.074	+0.058	−0.075
[25, 30)	0.492	+0.011	−0.011	+0.041	−0.045	+0.043	−0.047
[30, 35)	0.405	+0.009	−0.009	+0.034	−0.043	+0.035	−0.044
[35, 40)	0.325	+0.009	−0.009	+0.028	−0.034	+0.030	−0.035
[40, 45)	0.272	+0.008	−0.008	+0.024	−0.027	+0.026	−0.028
[45, 50)	0.282	+0.008	−0.008	+0.023	−0.027	+0.024	−0.028
[50, 55)	0.235	+0.007	−0.007	+0.023	−0.025	+0.025	−0.026
[55, 60)	0.194	+0.006	−0.006	+0.019	−0.024	+0.021	−0.024
[60, 65)	0.150	+0.006	−0.006	+0.015	−0.016	+0.016	−0.017
[65, 70)	0.102	+0.005	−0.005	+0.013	−0.012	+0.014	−0.013
[70, 75)	0.0836	+0.0041	−0.0041	+0.0103	−0.0087	+0.0111	−0.0096
[75, 80)	0.0748	+0.0036	−0.0036	+0.0087	−0.0086	+0.0094	−0.0093
[80, 90)	0.0521	+0.0021	−0.0021	+0.0059	−0.0056	+0.0063	−0.0059
[90, 100)	0.0381	+0.0017	−0.0017	+0.0043	−0.0036	+0.0047	−0.0040
[100, 110)	0.0239	+0.0013	−0.0013	+0.0028	−0.0023	+0.0031	−0.0026
[110, 120)	0.0175	+0.0011	−0.0011	+0.0024	−0.0016	+0.0027	−0.0019
[120, 130)	0.0106	+0.0009	−0.0009	+0.0015	−0.0011	+0.0017	−0.0014
[130, 140)	0.0090	+0.0008	−0.0008	+0.0012	−0.0008	+0.0015	−0.0012
[140, 150)	0.00646	+0.00064	−0.00064	+0.00089	−0.00063	+0.00110	−0.00090
[150, 175)	0.00333	+0.00031	−0.00031	+0.00047	−0.00039	+0.00056	−0.00049
[175, 200)	0.00195	+0.00023	−0.00023	+0.00025	−0.00017	+0.00034	−0.00028
[200, 250)	0.00077	+0.00010	−0.00010	+0.00012	−0.00008	+0.00016	−0.00013
[250, 500)	1.18e−04	+1.7e−05	−1.7e−05	+1.8e−05	−1.2e−05	+2.5e−05	−2.1e−05